Eulerian statistically preserved structures in passive scalar advection

Yoram Cohen,[1,2] Anna Pomyalov,[1] and Itamar Procaccia[1,2]
[1]*Department of Chemical Physics, The Weizmann Institute of Science, Rehovot 76100, Israel*
[2]*Department of Physics, the Chinese University of Hong Kong, Shatin, Hong Kong*
(Received 4 March 2003; published 4 September 2003)

We analyze numerically the time-dependent linear operators that govern the dynamics of Eulerian correlation functions of a decaying passive scalar advected by a stationary, forced two-dimensional Navier-Stokes turbulence. We show how to naturally discuss the dynamics in terms of effective compact operators that display Eulerian statistically preserved structures which determine the anomalous scaling of the correlation functions. In passing we point out a bonus of the present approach, in providing analytic predictions for the time-dependent correlation functions in decaying turbulent transport.

DOI: 10.1103/PhysRevE.68.036303 PACS number(s): 47.27.−i, 47.10.+g, 05.40.−a

I. INTRODUCTION

The aim of this paper is to discuss the statistical physics of turbulent advection of passive scalars [1]. We are interested in scalar fields $\theta(\boldsymbol{r},t)$ which are advected by a velocity field $\boldsymbol{u}(\boldsymbol{r},t)$ such that together they solve the set of equations

$$\frac{\partial \boldsymbol{u}}{\partial t}+(\boldsymbol{u}\cdot\boldsymbol{\nabla})\boldsymbol{u}=-\boldsymbol{\nabla}p+\nu\Delta\boldsymbol{u}+\boldsymbol{f}, \tag{1}$$

$$\frac{\partial \theta}{\partial t}+(\boldsymbol{u}\cdot\boldsymbol{\nabla})\,\theta=\kappa\Delta\,\theta+f. \tag{2}$$

In these equations $p(\boldsymbol{r},t)$, ν, and κ are the pressure field, the kinematic viscosity, and the scalar diffusivity, respectively. In this paper, the Navier-Stokes equations will be always forced with a time-stationary forcing $\boldsymbol{f}(\boldsymbol{r},t)$. The scalar field will be forced or unforced (decaying), depending on our interests below. We focus on the case of high Reynolds number Re and high Peclet number Pe, i.e., $\nu,\kappa\to 0$, where the turbulence of the velocity field is fully developed and where both fields display a significant range of scaling behavior at scales that are sufficiently far from the forcing scales.

A major theoretical question that had been answered recently has to do with the scaling properties of the correlation functions of the advected field [2,3]. Define the simultaneous many-point correlation function $F^{(N)}(\boldsymbol{r}_1,\ldots,\boldsymbol{r}_N)$ in the forced case by

$$F^{(N)}(\boldsymbol{r}_1,\ldots,\boldsymbol{r}_N)\equiv\langle\theta(\boldsymbol{r}_1,t)\,\theta(\boldsymbol{r}_2,t)\cdots\theta(\boldsymbol{r}_N,t)\rangle_f, \tag{3}$$

with $\langle\cdots\rangle_f$ denoting an average with respect to realizations of the stationary forcing $f(\boldsymbol{r},t)$ and of the velocity field $\boldsymbol{u}(\boldsymbol{r},t)$. It had been known for a long time that for high Re and Pe these functions are homogeneous functions of their arguments, i.e.,

$$F^{(N)}(\lambda\boldsymbol{r}_1,\ldots,\lambda\boldsymbol{r}_N)=\lambda^{\zeta_N}F^{(N)}(\boldsymbol{r}_1,\ldots\boldsymbol{r}_N), \tag{4}$$

with ζ_N being a scaling exponent that in general is *anomalous*, i.e., cannot be guessed from dimensional considerations. But only recently it became clear how these exponents are determined by the dynamical processes.

To understand the progress made, we rewrite the dynamical equation for $\theta(\boldsymbol{r},t)$ in the shorthand form

$$\frac{\partial\theta(\boldsymbol{r},t)}{\partial t}=\mathcal{L}\theta(\boldsymbol{r},t)+f(\boldsymbol{r},t), \tag{5}$$

where in the present case $\mathcal{L}\equiv\boldsymbol{u}\cdot\boldsymbol{\nabla}-\kappa\Delta$. In recent work [4,5] it was clarified why and how passive fields exhibit anomalous scaling, when the velocity field is a generic turbulent field. The key is to consider a *decaying problem* associated with Eq. (5), in which the forcing $f(\boldsymbol{r},t)$ is put to zero. The problem becomes then a linear initial value problem,

$$\partial\theta/\partial t=\mathcal{L}\theta, \tag{6}$$

with a formal solution

$$\theta(\boldsymbol{r},t)=\int d\boldsymbol{r}'R(\boldsymbol{r},\boldsymbol{r}',t)\,\theta(\boldsymbol{r}',0), \tag{7}$$

with the operator

$$R(\boldsymbol{r},\boldsymbol{r}',t)\equiv T^{+}\exp\left[\int_0^t ds\,\mathcal{L}(s)\right]\Bigg|_{\boldsymbol{r},\boldsymbol{r}'}, \tag{8}$$

and T^{+} being the time ordering operator. Define next the *time-dependent* correlation functions of the decaying problem:

$$C^{(N)}(\boldsymbol{r}_1,\ldots,\boldsymbol{r}_N,t)\equiv\langle\theta(\boldsymbol{r}_1,t)\cdots\theta(\boldsymbol{r}_N,t)\rangle. \tag{9}$$

Here pointed brackets without subscript f refer to the decaying object in which averaging is taken with respect to realizations of the velocity field and initial conditions. As a result of Eq. (7) the decaying correlation functions are evolved by a propagator $\mathcal{P}^{(N)}(\underline{\boldsymbol{r}},\underline{\boldsymbol{\rho}},t)$ (with $\underline{\boldsymbol{r}}\equiv\boldsymbol{r}_1,\boldsymbol{r}_2,\ldots,\boldsymbol{r}_N$ and $\underline{\boldsymbol{\rho}}\equiv\boldsymbol{\rho}_1,\boldsymbol{\rho}_2,\ldots,\boldsymbol{\rho}_N$):

$$C^{(N)}(\underline{\boldsymbol{r}},t)=\int d\underline{\boldsymbol{\rho}}\,\mathcal{P}^{(N)}(\underline{\boldsymbol{r}},\underline{\boldsymbol{\rho}},t)C^{(m)}(\underline{\boldsymbol{\rho}},0). \tag{10}$$

In writing this equation we made explicit use of the fact that the *initial* distribution of the passive field $\theta(\boldsymbol{r},0)$ is sta-

tistically independent of the advecting velocity field. Thus the operator $\mathcal{P}^{(N)}(\underline{\boldsymbol{r}},\underline{\boldsymbol{\rho}},t)$ can be written explicitly as

$$\mathcal{P}^{(N)}(\underline{\boldsymbol{r}},\underline{\boldsymbol{\rho}},t)\equiv\langle R(\boldsymbol{r}_1,\boldsymbol{\rho}_1,t)R(\boldsymbol{r}_2,\boldsymbol{\rho}_2,t)\cdots R(\boldsymbol{r}_N,\boldsymbol{\rho}_N,t)\rangle. \tag{11}$$

The key finding [4,5] is that the operator $\mathcal{P}^{(N)}(\boldsymbol{r},\boldsymbol{\rho},t)$ possesses a *left* eigenfunction of eigenvalue 1, i.e., there exists (for each N) a time-independent function $Z^{(N)}(\underline{\boldsymbol{r}})$ satisfying

$$Z^{(N)}(\underline{\boldsymbol{r}})=\int d\underline{\boldsymbol{\rho}}Z^{(N)}(\underline{\boldsymbol{\rho}})\mathcal{P}^{(N)}(\underline{\boldsymbol{r}},\underline{\boldsymbol{\rho}},t). \tag{12}$$

The functions $Z^{(N)}$ are referred to as ''statistically preserved structures,'' being invariant to the dynamics, even though *the operator is strongly time dependent and decaying*. How to form, from these functions, infinitely many conserved variables in the decaying problem was shown in Ref. [4], and is discussed again in Sec. III. The functions $Z^{(N)}(\boldsymbol{r})$ are homogeneous functions of their arguments, with anomalous scaling exponents ζ_N:

$$Z^{(N)}(\lambda\underline{\boldsymbol{r}})=\lambda^{\zeta_N}Z^{(N)}(\underline{\boldsymbol{r}})+\cdots, \tag{13}$$

where ''$\cdots$'' stand for subleading scaling terms. Since Eq. (12) contains $Z^{(N)}(\boldsymbol{r})$ on both sides, the scaling exponent ζ_N cannot be determined from dimensional considerations, and it can be anomalous. More importantly, it was shown that the correlation functions of the forced case, $F^{(N)}(\boldsymbol{r})$ Eq. (3), have exactly the same scaling exponents as $Z^{(N)}(\boldsymbol{r})$ [5]. In the scaling sense

$$F^{(N)}(\underline{\boldsymbol{r}})\sim Z^{(N)}(\underline{\boldsymbol{r}}). \tag{14}$$

This is how anomalous scaling in passive fields is understood.

Besides exactly soluble examples in which the advecting velocity field is nongeneric (i.e., δ-correlated in time) the existence of eigenfunctions of eigenvalue 1 of the time-dependent propagator was demonstrated fully only in shell models of turbulence. While the present authors believe that shell models contain a lot of the robust properties of real turbulence, this belief is not universally accepted in the community. It is therefore necessary to demonstrate that the mechanism sketched above exists indeed in the full problem, Eqs. (1) and (2). This had been done for third-order correlations within the Lagrangian formulation in Ref. [3]. The aim of this paper is to demonstrate this in the Eulerian frame, and for correlation functions of order 2, 4, and 6.

In Sec. II we describe the simulations of Eqs. (1) and (2) and the type of measurements that we performed. Section III is a theoretical digression, in which we analyze an exactly soluble simple model to guide ourselves as to how to analyze the numerical results to find the scaling forms of the nth-oder propagators and their eigenfunctions. Section IV describes the analysis of the data, and Sec. V offers a discussion and a summary of the paper.

II. SIMULATIONS

We performed a direct numerical simulation (DNS) of Eqs. (1) and (2) on a 2048×2048 two-dimensional(2D) array. The forcing $\boldsymbol{f}$ in Eq. (1) is random, δ-correlated in time, isotropic, and homogeneous. Its k dependence is

$$\langle|\boldsymbol{f}(\boldsymbol{k})|\rangle\propto k\exp[-0.5(k/1024)^2]. \tag{15}$$

This forcing is biased towards the small scales; this is done because of the inverse energy cascade that characterizes two-dimensional turbulence. The fluid dissipation is modeled by a hyperviscosity term proportional to $\Delta^8\boldsymbol{u}$. In addition we employed a ''friction'' term proportional to $\boldsymbol{u}$ in order to stabilize the velocity field on the largest scales. The passive field θ dissipates normally as shown in Eq. (2).

The simulations were performed for a decaying passive field θ, that is, the forcing f in Eq. (2) was put to zero. The initial conditions for the θ field were of the form

$$\tilde{\theta}(\boldsymbol{k},t=0)=\delta(k-k_0)\exp[i\gamma(\boldsymbol{k})], \tag{16}$$

where $\tilde{\theta}(\boldsymbol{k},t)$ is the Fourier transform of the real space variable defined as

$$\tilde{h}(\boldsymbol{k})=\frac{1}{2\pi}\int d\boldsymbol{r}h(\boldsymbol{r})e^{-i\boldsymbol{k}\cdot\boldsymbol{r}} \tag{17}$$

(from now on we will omit the tilde above the functions and denote the k space functions only by their variables). $\gamma(\boldsymbol{k})$ is a random variable in the interval $\gamma\in[0,2\pi]$ where $\gamma(\boldsymbol{k})=-\gamma(-\boldsymbol{k})$, ensuring that $\theta^*(-\boldsymbol{k},0)=\theta(\boldsymbol{k},0)$, and therefore that $\theta(\boldsymbol{r},t)$ is real.

As the initial conditions for θ and the forcing of the $\boldsymbol{u}$ fields are both homogeneous and isotropic so are the scalar correlation functions $C^{(N)}(\boldsymbol{r}_1,\cdots,\boldsymbol{r}_N,t)$ defined in Eq. (9), at all times t. We measured the $\boldsymbol{k}$ space correlation functions:

$$C^{(N)}(\boldsymbol{k}_1,\ldots,\boldsymbol{k}_N,t)\,\delta(\boldsymbol{k}_1+\cdots+\boldsymbol{k}_N)=\langle\theta(\boldsymbol{k}_1,t)\cdots\theta(\boldsymbol{k}_N,t)\rangle, \tag{18}$$

where again the average $\langle\cdots\rangle$ is over initial conditions and over realizations of the $\boldsymbol{u}$ field. The δ function appears due to translational invariance.

In accordance with Eq. (10) we define the $\boldsymbol{k}$ space propagator:

$$C^{(N)}(\underline{\boldsymbol{k}},t)=\int d\underline{\boldsymbol{k}}'\mathcal{P}^{(N)}(\underline{\boldsymbol{k}},\underline{\boldsymbol{k}}',t)C^{(N)}(\underline{\boldsymbol{k}}',0). \tag{19}$$

A. The two-point propagator

The only two-point correlator that is not zero is $C^{(2)}(\boldsymbol{k},-\boldsymbol{k},t)=\langle\theta(\boldsymbol{k})\theta^*(\boldsymbol{k})\rangle$. Because of the isotropy of the initial conditions and the driving field, the correlator depends only on the magnitude of $\boldsymbol{k}$. We can therefore consider the second-order structure function $S^{(2)}(k,t)=C^{(2)}(\boldsymbol{k},-\boldsymbol{k},t)$, and it propagator $\hat{\mathcal{P}}^{(2)}(k,k',t)$.

In discrete k space (as in our simulation on a grid) the propagator $\hat{\mathcal{P}}^{(2)}(k,k',t)$ has a matrix representation. For the

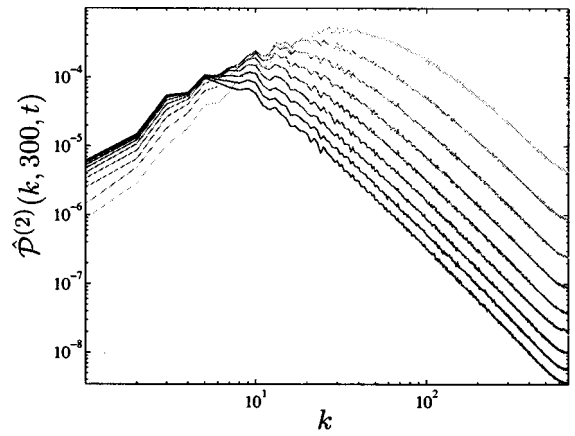

FIG. 1. $\hat{\mathcal{P}}^{(2)}(k,300,t)$ for nine different times. The first time is τ_{30}, i.e., the eddy turnover time at scale $k=30$, in lightest gray. Later times, in darker and darker grays, are at $2\tau_{30}$, $3\tau_{30}$, etc., until $9\tau_{30}$.

choice of initial conditions as in Eq. (16), $S^{(2)}(k,t)$ is simply the k_0th column of the propagator

$$S^{(2)}(k,t)=\int dk'\hat{\mathcal{P}}^{(2)}(k,k',t)S^{(2)}(k',0)=\hat{\mathcal{P}}^{(2)}(k,k_0,t). \tag{20}$$

In Fig. 1 we plot such a column of the two-point propagator, at nine different times. Two properties of the propagator should be noticed: as time progresses the overall amplitude decreases due to the decay, while the maximum moves from the initial k_0 to lower values of k. In Secs. III and IV we will find the scaling form of this propagator.

B. Multipoint propagators

In the case of the multipoint correlator the overall δ function and the isotropy of the fields do not reduce the dependence to a one-variable function. The propagators are therefore functions of many k vectors. It turns out however that measurement of the statistics for objects depending on many k vectors is very taxing. We opted therefore the extract from the DNS partial information on the dynamics of the $2N$-order structure functions with $N>1$:

$$S^{(2N)}(k,t)=\langle|\theta(\boldsymbol{k},t)|^{2N}\rangle. \tag{21}$$

Accordingly we define the reduced propagators:

$$S^{(2N)}(k,t)=\int dk'\hat{\mathcal{P}}^{(2N)}(k,k',t)S^{(2N)}(k',0). \tag{22}$$

We note that one does not expect single power laws for the fused $2N$-order structure functions with $N>1$; they generically include subleading contributions pertaining to products of lower order structure functions. Moreover, the reduced propagators are not Hermitian (the full ones are), and therefore do not lend themselves to direct eigenvalue-eigenfunction decomposition. We will therefore solve explicitly a simple model in the following section to learn how to think about the scaling properties of the fused propagators. The numerics show clearly that the qualitative features of the reduced propagators are the same as those seen in the second-order propagator, and therefore a scaling analysis is expected to be still useful. In Fig. 2 we present the numerical results for the fourth- and sixth-order reduced propagators, at the same 9 different times, stressing the similar qualitative behavior to that of the two-point propagator. We will learn in the following section how to think about the scaling properties of these objects and how to replot the numerical results in proper rescaled variables.

III. AN EXACTLY SOLVABLE CASE

In order to motivate the data analysis presented in Sec. IV we turn now to the Kraichnan model for passive scalar advection. The model is exactly solvable, and examining the analytic forms of the propagators offers clues to what should be expected in the generic case. In principle we could perform this analysis in terms of the Kraichnan model for a two-dimensional passive scalar. In fact, it is sufficient to consider the shell-model version; the latter is very transparent to analytic manipulations, and for our purposes the results throw equally useful light on how to perform the analysis of the DNS results.

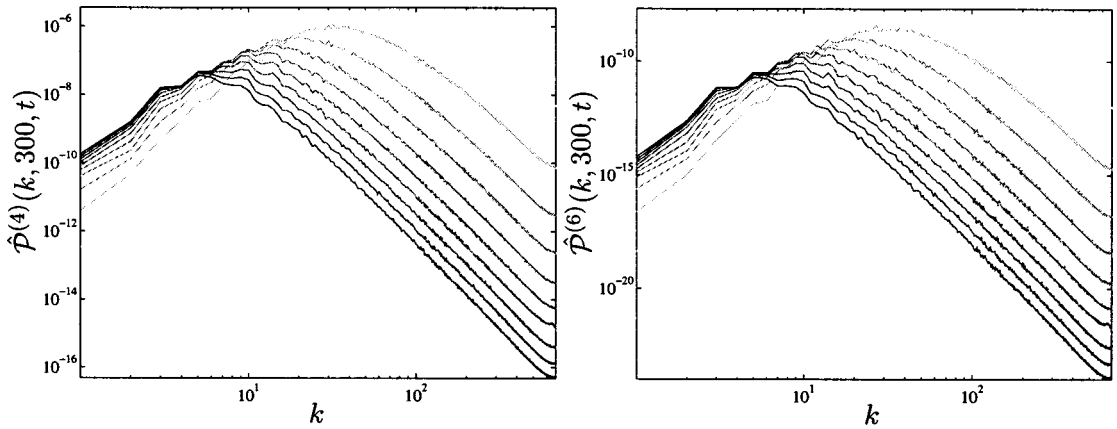

FIG. 2. $\hat{\mathcal{P}}^{(4)}(k,300,t)$ (upper panel) and $\hat{\mathcal{P}}^{(6)}(k,300,t)$ (lower panel) for the same nine different times as in Fig. 1.

A. The Kraichnan shell model

The Kraichnan shell model for passive scalar advection [4,6], as all other shell models of turbulent flows, is written in terms of Fourier components of the field. The Fourier components are restricted to shells denoted by the index m, and the equation takes on the form

$$\frac{d\theta_m}{dt}=\mathcal{L}_{m,n}\theta_n\,,$$

$$\mathcal{L}_{m,n}=ik_{m+1}u_{m+1}\delta_{m+1,n}+ik_m u_m^*\delta_{m-1,n}-\kappa k_m^2\delta_{m,n}\,. \tag{23}$$

Here k_m are the shell k vectors, $k_m=k_0\lambda^m$ for some k_0 and λ. The shell components of the velocity field, $u_m(t)$, are Gaussian random variables, δ-correlated in time, satisfying

$$\langle u_n(t)u_m^*(t')\rangle=c_0\,\delta_{n,m}\delta(t-t')\lambda^{-\xi m}. \tag{24}$$

Here ξ is the scaling exponent of the u field.

B. The second-order propagator

The second-order correlator satisfies the explicit equation (see Ref. [5])

$$\frac{d}{dt}S_n^{(2)}(t)=(M_{n,m}^{(2)}-\kappa k_n^2)S_m^{(2)}(t), \tag{25}$$

where $S_n^{(2)}(t)$ is the shell equivalent of the second-order structure function in Eq. (20),

$$S_n^{(2)}(t)=\langle|\theta_n(t)|^2\rangle. \tag{26}$$

The time evolution operator $\boldsymbol{M}^{(2)}$ has the form

$$M_{n,m}^{(2)}=(\alpha_n+\alpha_{n+1})\,\delta_{n,m}-\alpha_n\delta_{n-1,m}-\alpha_{n+1}\delta_{n+1,m}\,, \tag{27}$$

where

$$\alpha_n\equiv-c_0k_0^2\left\langle\frac{k_n}{k_0}\right\rangle^{\zeta_2}=-c_0k_0^2\lambda^{\zeta_2 n}, \tag{28}$$

and $\zeta_2=2-\xi$ is the dimensional scaling of the two-point correlation function. The operator $\boldsymbol{M}^{(2)}$ has the following useful scaling property:

$$\lambda^{-\zeta_2 p}M_{n+p,m+p}^{(2)}=M_{n,m}^{(2)}\,. \tag{29}$$

The second-order propagator has, in the limit of vanishing viscosity, the explicit form

$$\mathcal{P}_{n|m}^{(2)}(t)=\exp(t\boldsymbol{M}^{(2)})|_{n,m}\,. \tag{30}$$

Note that the time evolution operator and the propagator are both Hermitian, and thus admit an eigenvector decomposition. The time evolution operator has two types of eigenvectors $\psi_n^{(2,q)}$ and $\tilde{\psi}_n^{(2,q)}$ which we can regard as slow modes and fast modes, respectively. Here the index k stands for the eigenmode index. The fast modes are dominated by the viscous term, their support is in the viscous range, and they can essentially be taken to be $\tilde{\psi}_n^{(2,q)}=\delta_{n,q}$ for some shell q with the shell index $q>m_d$, above which viscosity dominates Eq. (25). The transition shell m_d is determined by the condition $\kappa k_{m_d}^2=c_0k_{m_d}^{\zeta_2}$. For the fast modes we have the following approximate equation:

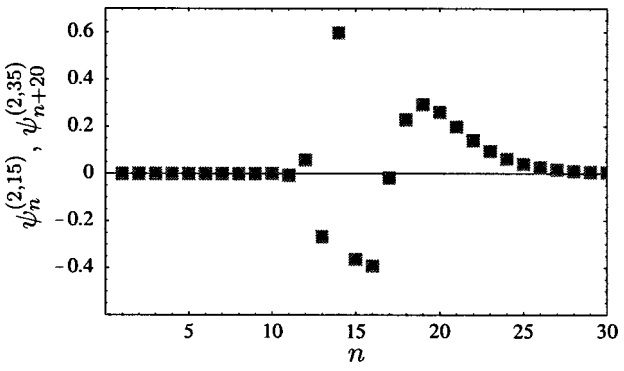

FIG. 3. A plot of the eigenvectors $\psi_n^{2,15}$ (squares) and $\psi_{n+20}^{2,35}$ (triangles), for $n\in[0,30]$.

$$\frac{d}{dt}\tilde{\psi}_n^{(2,q)}=-\kappa k_n^2\tilde{\psi}_n^{(2,q)}\,, \tag{31}$$

therefore their eigenvalues are $\beta_q=-\kappa k_q^2$.

For slow modes $\psi_n^{(2,q)}$, which have their support on shells smaller than m_d, the dissipative term can be neglected and they satisfy an eigenfunction equation of the form

$$\beta_q\psi_n^{(2,q)}=M_{n,m}^{(2)}\psi_m^{(2,q)}\,. \tag{32}$$

For a sufficiently large inertial range we can use the scaling property (29) to get

$$\beta_q\psi_n^{(2,q)}=\lambda^{-\zeta_2 p}M_{n+p,m+p}^{(2)}\psi_m^{(2,q)}\,. \tag{33}$$

Shifting indices we rewrite

$$\beta_q\psi_{n-p}^{(2,q)}=\lambda^{-\zeta_2 p}M_{n,m}^{(2)}\psi_{m-p}^{(2,q)}\,. \tag{34}$$

Defining now a vector

$$\chi_n\equiv\psi_{n-p}^{(2,q)}\,, \tag{35}$$

we have

$$\lambda^{\zeta_2 p}\beta_q\chi_n=M_{n,m}^{(2)}\chi_m\,. \tag{36}$$

We can thus define $\psi_n^{(2,q+p)}\equiv\chi_n$, an eigenfunction of the time evolution operator $\boldsymbol{M}^{(2)}$ with eigenvalue $\lambda^{\zeta_2 p}\beta_q$.

We can therefore conclude that the eigenvectors and eigenvalues may be obtained from each other by shift of the indices:

$$\psi_{n+p}^{(2,q+p)}=\psi_n^{(2,q)}\,, \tag{37}$$

$$\beta_{q+p}=\lambda^{\zeta_2 p}\beta_q\,. \tag{38}$$

Figure 3 demonstrates that indeed two different eigen-

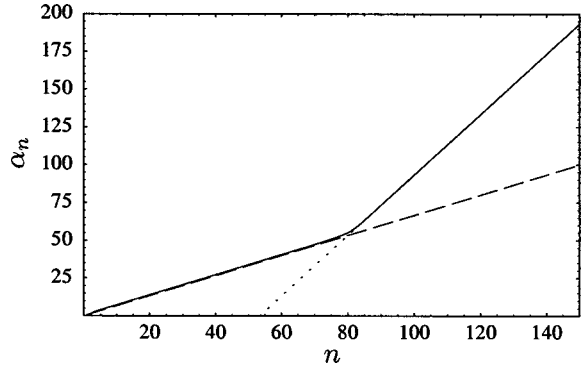

FIG. 4. The eigenvalues, plotted from small to large. The eigenvalues are well fitted by the analytic predictions $k_m^{\zeta_2}$ (dashed line), for the slow modes, and by k_m^2 (dotted line) for the fast modes. The transition to the viscous range occurs at shell $m_d=80$.

functions coincide once shifted with respect to each other. It follows from Eq. (38) that

$$\beta_q \propto \alpha_q . \tag{39}$$

In Fig. 4 the spectrum of the eigenvalues is plotted, showing the two expected regions: a region for which the scaling of the eigenvalues is $\propto k_n^{\zeta_2}$ for the slow modes, and $\propto k_n^2$ for the fast modes.

The lowest eigenvalue is proportional to α_0. The eigenfunction $\psi_n^{(2,0)}$ associated with it can be calculated explicitly, and it exhibits a normal, dimensional, scaling in the inertial range:

$$\psi_n^{(2,0)} \propto (k_n/k_0)^{-\zeta_2}. \tag{40}$$

Using Eqs. (37) and (40), which imply that $\psi_n^{(2,q)}$ has a scaling ''tail'' with exponent ζ_2, starting after shell q we establish

$$\psi_n^{(2,q)} \propto (k_n/k_q)^{-\zeta_2} \propto \alpha_q/\alpha_n , \; q<n<m_d . \tag{41}$$

We now use these results to learn how to rescale our numerical data. Suppose that we started with an initial condition in some shell n in the inertial range, $S_p^{(2)}(0)=\delta_{p,n}$. The fast modes do not contribute significantly to the time dependence, since they decay fast and anyhow have no support in the inertial range. Thus, using only the slow modes and Eqs. (27) and (30), we have, for $p<n$,

$$S_p^{(2)}(t) = \sum_{q=1}^{p} \psi_n^{(2,q)} e^{\alpha_q t} \psi_p^{(2,q)} \propto \frac{1}{\alpha_p \alpha_n} \sum_{q=1}^{p} \alpha_q^2 e^{\alpha_q t} \propto \mathcal{P}_{p|n}^{(2)}(t). \tag{42}$$

In going from the first to the second line we inserted the δ-function initial conditions, getting thus a column of the propagator $\mathcal{P}_{p|n}^{(2)}(t)$. Remember that in our DNS calculations we fixed the column index, and are interested in the scaling behavior with respect to the row index and time. Therefore we compute now (up to an overall dimensional constant)

$$\begin{aligned}
\lambda^{\zeta_2 m}\mathcal{P}_{p-m|n}^{(2)}(\lambda^{\zeta_2 m}t) &= \frac{\lambda^{\zeta_2 m}}{\alpha_{p-m}\alpha_n} \sum_{q=1}^{p-m} \alpha_q^2 e^{\alpha_{q+m} t} \\
&= \frac{1}{\alpha_p \alpha_n} \sum_{q=1}^{p-m} \alpha_{q+m}^2 e^{\alpha_{q+m} t} \\
&= \frac{1}{\alpha_p \alpha_n} \sum_{q=m+1}^{p} \alpha_q^2 e^{\alpha_q t} \\
&= \mathcal{P}_{p|n}^{(2)}(t) - \frac{\alpha_m}{\alpha_p}\mathcal{P}_{m|n}^{(2)}(t),
\end{aligned} \tag{43}$$

where we have used the explicit form of the propagator in Eqs. (42) and (28). For m much smaller than p we can neglect the second term. Then we conclude that the propagator is a homogeneous function of the variables k_p and t. Explicitly, multiplying by t,

$$t\mathcal{P}^{(2)}(k_p,k_n,t) = (\lambda^{-\zeta_2 m}t)\mathcal{P}^{(2)}(\lambda^m k_p, k_n, \lambda^{-\zeta_2 m}t). \tag{44}$$

For fixed k_n this is a homogeneous function of two arguments which can be always written in the form

$$\mathcal{P}^{(2)}(k_p,k_n,t) = \frac{\text{const}}{\alpha_n t}\Lambda(\alpha_p t), \tag{45}$$

for some function $\Lambda(x)$. The symmetry between p and n is restored by realizing that the asymptotic form of $\Lambda(x)$ is $1/x$ for large x.

This scaling form was also found in the study of the generic shell models of passive scalar advection (arbitrary time dependence in the velocity correlations) [5] and we will show that the same scaling form survives when we go back to the generic model studied by DNS.

C. The multipoint propagators

The invariance of Eq. (23) under a uniform phase change $\theta_n \to e^{i\phi}\theta_n$ dictates that the only nonzero correlation functions will have an equal number of variables θ_n and conjugated variables θ_m^*. We define

$$C_{i_1,\ldots,i_m,j_1,\ldots,j_N}^{(2N)}(t) = \langle \theta_{i_1}(t)\cdots\theta_{i_N}(t)\,\theta_{j_1}^*(t)\cdots\theta_{j_N}^*(t)\rangle. \tag{46}$$

As in the two-point case we can define the respective multipoint differential time derivative operator, analogous to Eq. (25). In the limit of vanishing viscosity,

$$\frac{d}{dt}C_{\underline{i},\underline{j}}^{(2N)}(t) = M_{\underline{i},\underline{j}|\underline{i}',\underline{j}'}^{(2N)} C_{\underline{i}',\underline{j}'}^{(2N)}(t). \tag{47}$$

The respective propagator is defined by

$$C_{\underline{i},\underline{j}}^{(2N)}(t) = \mathcal{P}_{\underline{i},\underline{j}|\underline{i}',\underline{j}'}^{(2N)}(t) C_{\underline{i}',\underline{j}'}^{(2N)}(0), \tag{48}$$

$$\mathcal{P}_{\underline{i},\underline{j}|\underline{i}',\underline{j}'}^{(2N)} = \exp(t\boldsymbol{M}^{(2N)})\big|_{\underline{i},\underline{j}|\underline{i}',\underline{j}'} . \tag{49}$$

Because of the time reversibility of the statistics of the $\boldsymbol{u}$ fields, and the antihermiticity of the unaveraged differential operator $\mathcal{L}$ in Eq. (23), $\mathcal{L}^*_{m,n} = -\mathcal{L}_{n,m}$, both the time derivative operator $\boldsymbol{M}^{(2N)}$ and the propagator itself are Hermitian, and therefore admit eigenvalue decomposition. Furthermore the operator $\boldsymbol{M}^{(2N)}$ has the following scaling property:

$$M^{(2N)}_{\underline{i},\underline{j}|\underline{i}',\underline{j}'} = \lambda^{-\zeta_2 p} M^{(2N)}_{\underline{i}+p,\underline{j}+p|\underline{i}'+p,\underline{j}'+p}. \tag{50}$$

As in the two-point case the dynamics within the scaling range is determined by slow modes,

$$\beta^{(2N,l)}_k \psi^{(2N,l,k)}_{\underline{i},\underline{j}} = M^{(2N)}_{\underline{i},\underline{j}|\underline{i}',\underline{j}'} \psi^{(2N,l,k)}_{\underline{i}',\underline{j}'}. \tag{51}$$

In this equation the index l stands for a family of eigenmodes, and k for their index within the family. Each l family can be obtained from any one of its members by shifting the indices. The eigenvalues of the modes within a given family can be obtained also by a shift,

$$\psi^{(2N,l,k+p)}_{\underline{i}+p,\underline{j}+p} = \psi^{(2N,l,k)}_{\underline{i},\underline{j}}, \tag{52}$$

$$\beta^{(2N,l)}_{k+p} = \lambda^{\zeta_2 p} \beta^{(2N,l)}_k. \tag{53}$$

Note that in the two-point case we had only one family of eigenmodes. Here we added the index l to the eigenvalues and eigenmodes to distinguish the different families. Note also that in Eq. (53) the scaling exponent of the eigenvalues is ζ_2; this stems from the scaling properties of the differential operator $\boldsymbol{M}^{(2N)}$, cf. Eq. (50). However, the eigenmodes display in general anomalous scaling which can be represented by

$$\psi^{(2N,l,k)}_{\underline{i},\underline{j}} = \lambda^{-p\,\zeta_{2N,l}}\, \psi^{(2N,l,k)}_{\underline{i}+p,\underline{j}+p}, \tag{54}$$

where $\zeta_{2N,l}$ is the (anomalous) scaling exponent of the lth family of eigenmodes.

Since the DNS's were analyzed in terms of fused objects, we focus on initial conditions in Eq. (48) for which all the $2N$ indices are the same. We also measure the resulting structure functions

$$S^{(2N)}_n = \langle |\theta_n|^{2N} \rangle. \tag{55}$$

This procedure will extract a fused propagator for which there are only two indices, and we denote it below as $\mathcal{P}^{(2N)}_{p|n}(t)$. This propagator is not Hermitian, it has in general no eigenfunction decomposition, but we can understand the scaling form of any of its columns from the knowledge of the full propagator and its eigenfunctions.

The equivalent of Eq. (42) for $S^{(2N)}_k(t=0) = \delta_{k,n}$, $p<n$, summing over all families of slow modes (i.e., over the index l) is

$$\begin{aligned} S^{(2N)}_p(t) &= \sum_l \sum_{q=1}^{p} \psi^{(2N,l,q)}_n e^{\alpha_q t} \psi^{(2N,l,q)}_p \\ &= \sum_l \frac{C_l}{(\alpha_p \alpha_n)^{\frac{\zeta_{2N,l}}{\zeta_2}}} \sum_{q=1}^{p} \alpha_q^{(2\zeta_{2N,l}/\zeta_2)} e^{\alpha_q t} = \mathcal{P}^{(2N)}_{p|n}(t). \end{aligned} \tag{56}$$

In going from the first to the second line we have used the fact that

$$\psi^{2N,l,p}_{i,i,\ldots,i} \propto \left(\frac{\alpha_i}{\alpha_p}\right)^{-\zeta_{2N,l}/\zeta_2}. \tag{57}$$

This follows directly from Eqs. (52) and (54).

Using the same argumentation as in Eq. (43), we get

$$\mathcal{P}^{(2N)}_{p|n}(t) = \sum_l \frac{C_l}{(\alpha_n t)^{\zeta_{2N,l}/\zeta_2}} \Lambda^{(2N,l)}(\alpha_p t), \tag{58}$$

where again the C_l's are dimensional constants and the functions $\Lambda^{(2N,l)}(x)$ are some functions with the asymptotic form $\Lambda^{(2N,l)}(x) \approx x^{-\zeta_{2N,l}/\zeta_2}$ for x large. We note that for sufficiently long times and if the scaling exponents are well separated, we can expect the sum to be dominated by the leading scaling exponent.

IV. DATA ANALYSIS

The detailed analysis that was possible for the simple model of Sec. III is not available for the generic model, Eqs. (1) and (2). Our strategy is to assume that the scaling forms derived in the last section are still valid for the generic model, and to demonstrate this by replotting the data accordingly. We will see that these predictions are born out by the data.

A. analysis of the two-point propagator

In light of Eq. (44), we expect the second-order propagator $\hat{\mathcal{P}}^{(2)}(k,k_0,t)$ to be, for a fixed k_0, a homogeneous function of the variable kt^{1/ζ_2}, and to decay as $1/t$:

$$\hat{\mathcal{P}}^{(2)}(k,k_0,t) \propto \frac{1}{t} H^{(2)}(kt^{1/\zeta_2}), \tag{59}$$

where $H^{(2)}$ is some function. We test the correctness of this form in Fig. 5. To this aim we replot that data shown in Fig. 1 in different coordinates, multiplied by t and as a function of

$$\hat{k} = kt^{1/\zeta_2}. \tag{60}$$

The quality of the data collapse appears to strongly support the proposed scaling form. We note that the data collapse is superior on the right of the maximum, and less convincing at its left. We believe that this stems from two reasons. First, there is better statistics for the right part of the curve, simply because it belongs to larger k vectors where the angular av-

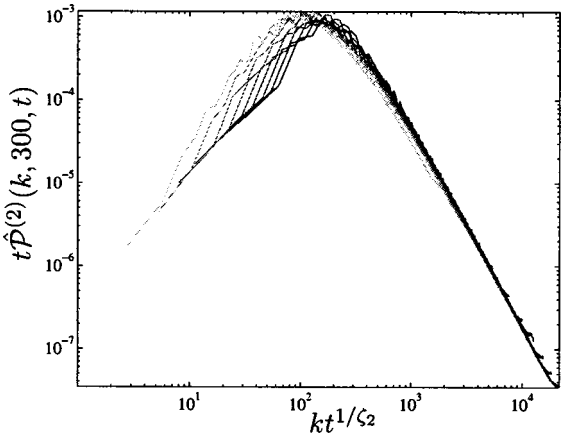

FIG. 5. $t\hat{\mathcal{P}}^{(2)}(k,300,t)$ for nine different times (light gray, earliest; dark gray, last).

erage is more extensive. Second, the left part of the curve is more sensitive to the finite-size effects, particularly to the fact that the driving velocity field loses its scaling form close to L. With all the limitations of the numerical simulations we consider the data collapse as very satisfactory.

If the prediction for the two-point function holds, then we will have the following for the time-dependent integral:

$$\int_0^\infty \hat{\mathcal{P}}^{(2)}(k,k',t)dk \approx \frac{1}{t^{1+1/\zeta_2}} \int_0^\infty H^{(2)}(\hat{k})d\hat{k} \propto \frac{1}{t^{1+1/\zeta_2}}. \tag{61}$$

In Fig. 6, we show that indeed after an initial period the integral settles on a scaling form consistent with Eq. (61).

Using the form of the propagator we can establish the existence of a left eigenmode of eigenvalue 1 of the two-point propagator. Integrating over the two sides of Eq. (12) we have a time-independent expression on the left-hand side. We therefore expect that the weighted integral of the propagator with the function $Z^{(2)}$ will be constant:

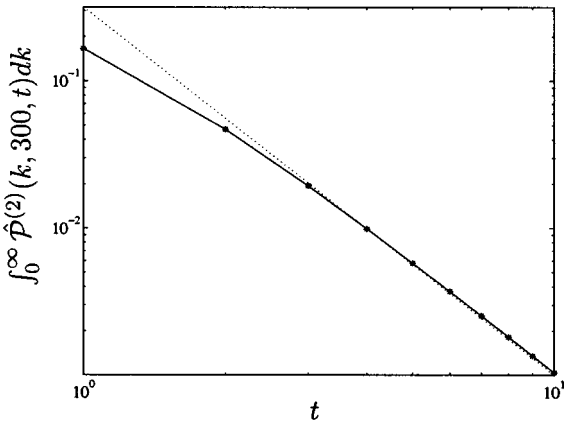

FIG. 6. The integral of the two-point propagator, $\int_0^\infty \hat{\mathcal{P}}^{(2)}(k,300,t)d^2k$, (solid line) as a function of time. The dotted line is the expected $t^{-(1+1/\zeta_2)}$ (time is measured in this figure, and in the ones that follow, in units of τ_{30}, the eddy turnover time of $k=30$).

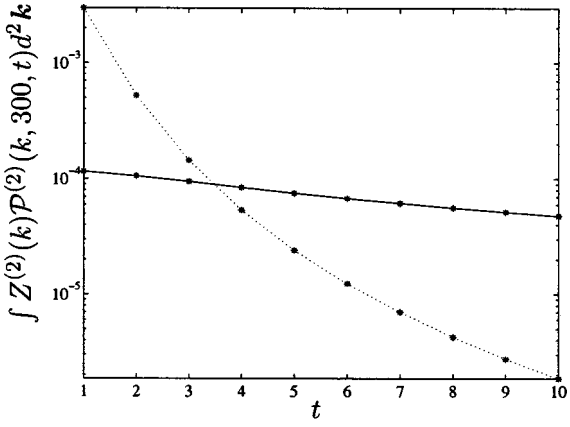

FIG. 7. The integral of the two-point propagator $P^{(2)}(k,300,t)$ weighed by the left zero mode $Z^{(2)}(k)$ (solid line), compared to the integral of the unweighted second-order structure function (dotted line).

$$\int Z^{(2)}(\boldsymbol{k})\mathcal{P}^{(2)}(\boldsymbol{k},\boldsymbol{k}',t)d^2\boldsymbol{k} \propto \int_0^\infty k^{-2-\zeta_2}\frac{H^{(2)}(kt^{1/\zeta_2})}{t}kdk = \int_0^\infty \frac{H(\hat{k})}{\hat{k}^{1+\zeta_2}}d\hat{k} = \text{const}, \tag{62}$$

where we have used the fact that in an isotropic two-dimensional system we have $Z^{(2)}(\boldsymbol{k}) \sim F^{(2)}(\boldsymbol{k}) \propto k^{-2-\zeta_2}$. We note that the constancy of this integral should be judged on the background of the decaying function, as done in Fig. 7. We see that while the second-order structure function decays over three orders of magnitude, the ''constant'' objects change by a factor of 2. The lack of constancy can be attributed to the sensitivity to the outer scale as seen in the data collapse in Fig. 5. If the collapse on the left side of the curve were perfect, so would be the constancy of the weighted integral. Note that in the calculation we have employed $\zeta_2 = 0.67$ in agreement with Ref. [7].

B. Analysis of the multipoint propagators

Examining Eq. (58), we expect that for long times the functional form of the propagator for the fused correlation function defined in Eq. (22) is

$$\hat{\mathcal{P}}^{(2N)}(k,k',t) \propto \frac{1}{t^{\zeta_{2N}/\zeta_2}} H^{(2N)}(kt^{1/\zeta_2}), \tag{63}$$

where ζ_{2N} is the leading scaling exponent for the $2N$th correlation function. In Fig. 8 we demonstrate the data collapse obtained by assuming this form for the fourth- and sixth-order propagators. We notice the same excellent collapse on the right-hand side of the function as in the second-order propagator. Also the problems with the outer scale show up in a similar manner, giving less than impressive collapse of the left hand part of the function. For the present data collapse we employed simple scaling $\zeta_{2N} = N\zeta_2$; our data do not support strongly anomalous exponents. We should stress

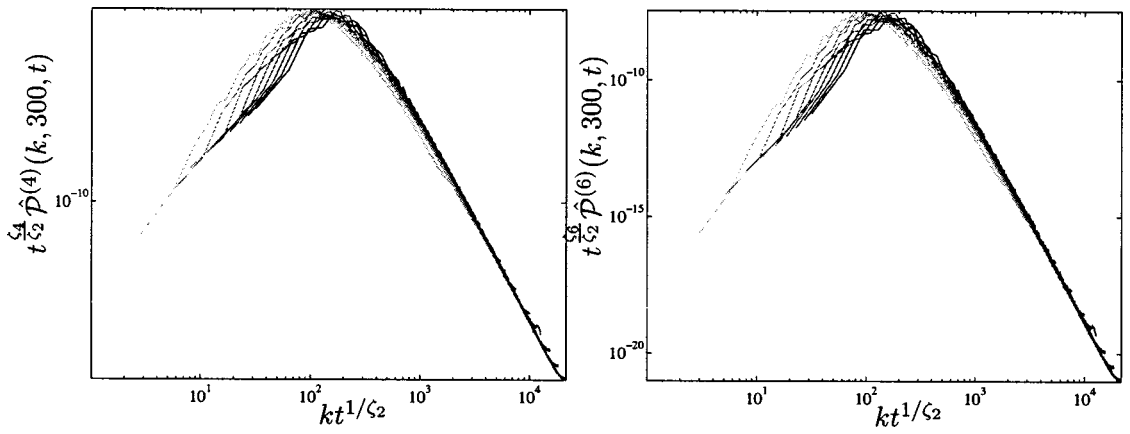

FIG. 8. $t^{\zeta_4/\zeta_2}\hat{\mathcal{P}}^{(4)}(k,300,t)$ (upper panel) and $t^{\zeta_6/\zeta_2}\hat{\mathcal{P}}^{(6)}(k,300,t)$ (lower panel) for nine different times (light gray, earliest; dark gray, last).

however that the relatively short scaling range does not allow a definite statement about the normality vs the anomaly of the scaling exponents.

Using the form of the fused multipoint correlators we can again predict the time behavior of their integral:

$$\int_0^\infty \hat{\mathcal{P}}^{(2N)}(k,k',t)dk \approx \frac{1}{t^{(1+\zeta_{2N})/\zeta_2}} \int_0^\infty H(\hat{k})d\hat{k} \propto \frac{1}{t^{(1+\zeta_{2N})/\zeta_2}}. \tag{64}$$

In Fig. 9 the time dependence of the integrals is plotted, showing agreement of similar quality to Fig. 6.

As in the two-point case, weighing the fused multipoint functions by the appropriate multipoint fused steady state correlators should yield a constant:

$$\int Z^{(2N)}(k)\hat{\mathcal{P}}^{(2N)}(k,k',t)d^2\boldsymbol{k} \propto \int_0^\infty \frac{H^{(2N)}(kt^{1/\zeta_2})}{k^{2+\zeta_{2N}}t^{\zeta_{2N}/\zeta_2}}kdk = \int_0^\infty \frac{H^{(2N)}(\hat{k})}{\hat{k}^{1+\zeta_{2N}}}d\hat{k} = \text{const}, \tag{65}$$

where $Z^{2N}(k) \propto k^{-2-\zeta_{2N}}$. The quality of the constancy is demonstrated in Fig. 10. Again finite-size effects lead to some decrease in time of these weighted objects, which nevertheless is very much reduced compared to the decaying correlation functions.

V. CONCLUDING REMARKS

We have demonstrated in this paper that the generic advection of a passive scalar by a velocity field that obeys the Navier-Stokes equations can be discussed in terms of Eulerian statistically preserved structures. By initiating a decay with δ-function initial conditions (concentrated on $k=300$) we have found numerically the corresponding columns of the time-dependent propagators for the second-, fourth- and sixth-order correlation functions [where for the fourth- and sixth-order objects we considered partial (''fused'') information]. Note that in contrast to the Lagrangian formulation of statistically preserved structures [3], for which there is no preserved structure corresponding to the second-order correlation, in the Eulerian formulation such an object exists and had been analyzed explicitly. We have used a simple (nongeneric) model of passive scalar advection to guess the analytic scaling form of the propagators in the generic problem.

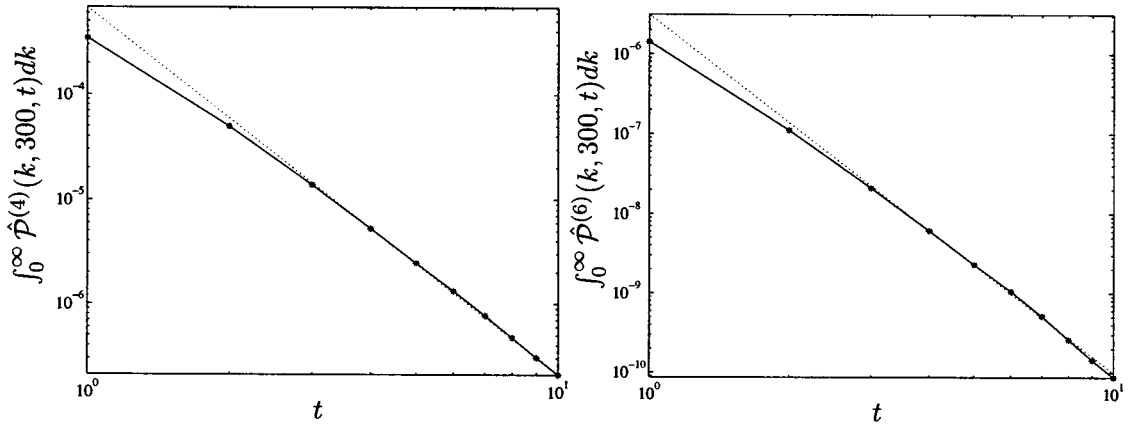

FIG. 9. The integral of the four-point (upper panel) and six-point (lower panel) propagators (solid line), $\int_0^\infty \hat{\mathcal{P}}^{(2m)}(k,300,t)d^2k$, compared with the expected $t^{-(1+\zeta_{2N})/\zeta_2}$ (dotted line).

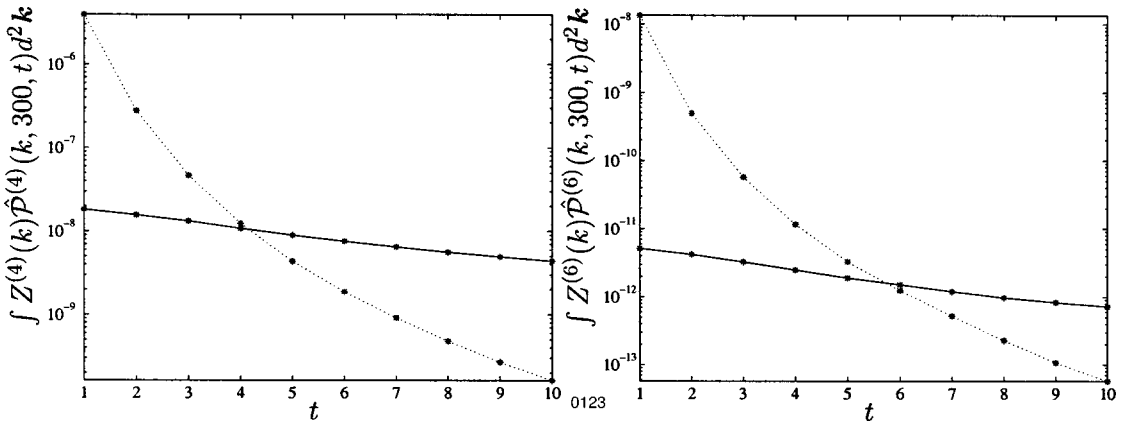

FIG. 10. The integral of the four-point propagator $P^{(4)}(k,300,t)$ (upper panel) and the six-point propagator $P^{(6)}(k,300,t)$ weighted by the left zero modes $Z^{(4)}(k)$ and $Z^{(6)}(k)$, respectively (solid line) compared to the integral of the unweighted object (dotted line).

The test for the relevance of this guessed form is the data collapse shown in Figs. 5 and 8. The guessed time dependence appears to be in close correspondence with the data as shown in Figs. 6 and 9.

The analytic forms of the propagators predict the existence of eigenmodes with eigenvalue 1 (statistically preserved structures). We believe that this is an important demonstration of Eulerian statistically preserved structures in a generic flow. The numerical evidence for the constancy of the latter is encouraging, if not fully conclusive, as seen in Figs. 7 and 10. We attributed the (relatively small) decrease in amplitude of the putative statistically preserved structures to the less than perfect data collapse at the largest scales (smallest k vectors) that are seen in Figs. 5 and 8. These in turn stem from the intervention of the outer scale in our scaling range, a boundary effect that we did not succeed to eliminate in our modest-size simulations. It would be interesting to see whether larger 2D simulations could remove this finite-size effect to demonstrate conclusively the constancy of the statistically preserved structures. In addition, larger scaling ranges in improved numerics will help to distinguish better between normal and anomalous scaling exponents.

In concluding we wish to point out an additional benefit to the present formulation. Usually in modeling turbulent advection it is customary to resort to dubious concepts such as 'turbulent diffusion' in order to write a diffusion equation for the correlation functions. The present approach indicates a much better procedure, i.e., to find, for a given turbulent field, the form of the propagator which can be then used to provide analytic predictions for any initial ($t=0$) correlation function. This procedure may be quite interesting for more complex hydrodynamic flows with unusual boundaries or coherent structures. We believe that when the turbulence is sufficiently well developed scaling forms for the propagator will exist, and once found can be used to solve efficiently any statistical initial value problem.

ACKNOWLEDGMENTS

We thank Antonio Celani for providing us with his code for DNS of two-dimensional turbulent advection. This work had been supported in part by the European Commission under a TMR grant, the Minerva Foundation, Munich, Germany, and the Naftali and Anna Backenroth-Bronicki Fund for Research in Chaos and Complexity.

[1] A. S. Monin and A. M. Yaglom, *Statistical Fluid Mechanics* (MIT, Cambridge, MA, 1979), Vol. 1, Chap. 5.
[2] D. Bernard, K. Gawedzki, and A. Kupiainen, J. Stat. Phys. **90**, 519 (1998).
[3] A. Celani and M. Vergassola, Phys. Rev. Lett. **86**, 424 (2001).
[4] I. Arad, L. Biferale, A. Celani, I. Procaccia, and M. Vergassola, Phys. Rev. Lett. **87**, 164502 (2001).
[5] Y. Cohen, T. Gilbert, and I. Procaccia, Phys. Rev. E **65**, 026314 (2002).
[6] R. Benzi, L. Biferale, and A. Wirth, Phys. Rev. Lett. **78**, 4926 (1997).
[7] A. Celani A. Lanotte A. Mazzino, and M. Vergassola, Phys. Rev. Lett. **84**, 2385 (2000).